Scientia Iranica A (2014) 21(4), 1297–1308

SCIENTIA IRANICA

Sharif University of Technology
**Scientia Iranica**
*Transactions A: Civil Engineering*
www.scientiairanica.com

# Shape optimization of concrete arch dams considering abutment stability

**M. Takalloozadeh and M. Ghaemian***

*Department of Civil Engineering, Sharif University of Technology, Tehran, Iran.*

Received 17 March 2013; received in revised form 27 August 2013; accepted 24 September 2013

**KEYWORDS**
Shape optimization; Concrete arch dam; Abutment stability; Minimum weight design.

**Abstract.** A novel and robust approach is proposed to find the optimum shape of concrete arch dams located on any unsymmetrical shape of a valley. The approach is capable of finding the optimum shape for any given valley type in suitable time, based on abutment stability analysis, against thrust forces from an arch dam. The behavior and stability of a concrete arch dam is strongly dependent on the bedrock on which the dam rests. The stability of the abutment is considered a constraint in the proposed approach. In addition, a new objective function is introduced to decrease the final volume of the arch dam. Furthermore, a computer program was developed, which takes the effect of the dam foundation system into consideration, and can model most loads applicable to arch dams. The optimization problem is solved via both Particle Swarm Optimization (PSO) and classical methods. Several practical factors have been considered to make the approach more feasible and effective in practical projects. The results show the efficiency of the proposed method and the final shape satisfies all constraints.



## 1. Introduction

Shape optimization has received a great deal of attention from engineers over the last decade and plays an important role in the design of arch dams. Shape optimization of concrete arch dams has been the subject of much research for over 50 years. It started with the work of Rajan [1], as part of his PhD thesis in 1968, and was continued by several other researchers [2-5]. One comprehensive research in this field was undertaken by Bofang [6-8], in which a computer code was developed to include several parameters as design variables for the purpose of practical design.

Shape optimization of concrete arch dams can be time consuming, due to the large amount of time required for dam analysis in the process of optimization. The main challenge in shape optimization of concrete arch dams is the presence of several local minima in optimization space, and the difficulty in convergence to a global minimum.

In recent years, several authors have utilized intelligence methods to overcome these challenges [9-13]. Several methods in shape sensitivity analysis are used to decrease optimization processing time [8,14,15]. This field of research continued, considering seismic load, to complete the modeling of a dam [12,16] and to find the global optimum in less time [17-19].

An arch dam is a structure where large forces are applied to the bedrock at both banks compared to other types of dam. Abutment stability in arch dams is important and must be investigated during design stages. Arch dams have failed in the past. But, as far as is known, it has never been because of dam body failure, which has always been attributed to the foundation [20]. Therefore, in the optimization process, the effect of abutment stability analysis must be considered. We include the thrust forces of the dam on the wedges at the abutment for the purpose of their stability, and the factor of safety against

*. *Corresponding author.*
*E-mail address: ghaemian@sharif.edu (M. Ghaemian)*

sliding is imported in the optimization process as a constraint.

In this study, shape optimization of concrete arch dams based on abutment stability was investigated. Only wedges in contact with the dam body are considered for the purpose of the analysis. The PSO algorithm, combined with approximate analysis and a classical method of optimization such as the exterior penalty method and gradient descent, combined with the finite element method, is used to perform shape optimization.

## 2. Problem definition

In general, the best shape for arch dam is the one which reduces bending and twisting side effects, makes uniform compressive stresses and limits tensile stresses under all loadings. Arch dam optimization design belongs to complex optimization problems. In the optimization process, the object function and constraint conditions are nonlinear functions [20].

Shape optimization can be formulated in different ways. However, for a typical valley, shape such as Figure 1, one can write the problem of the shape optimization of arch dams in mathematical form as follows:

$$\text{Find} \quad T = T(x,z) \quad \text{and} \quad y = y(x,z). \tag{1a}$$

$$\text{Minimize} \quad V, \tag{1b}$$

Subject to:

$$g_i \leq 0 \quad i = 1,2,...,m, \tag{1c}$$

and:

$$h_j = 0 \quad j = 1,2,...,p, \tag{1d}$$

in which, $V$ stands for the volume of the dam, $T$ is designated as the thickness of the dam, and $y$ represents the $y$ coordinate of the upstream face of the dam. $g$ and h are the inequality and equality constraints, respectively.

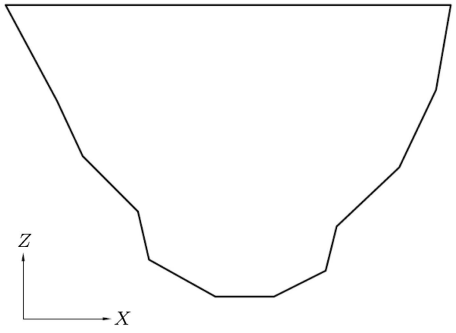


**Figure 1.** Typical valley section in concrete arch dams.

### 2.1. Objective function and design variables

The cost of concrete is nearly 50% of the total cost of civil work, excluding hydro mechanical equipment [20]. Thus, it is not irrational to consider it an objective function.

Shape optimization can improve as more design variables are included, but it increases the cost of calculation. In this research, 30 parameters were considered as design variables.

A parabolic function is used to define the upstream face of the crown cantilever based on three variables as the coordinates of crest, base and mid height. Four variables are defined to determine the thickness of the crown cantilever, as shown in Figure 2. Thickness variation along the height of the dam is cubic.

To define the horizontal section, it is divided into two parts: left and right (Figure 3). This is done in order to model an unsymmetrical arch dam. Each side is divided into two segments: constant thickness and variable thickness. The thickness of the dam in the horizontal section is constant in the first segment and increases by a parabolic function in the second. The thickness of the segment in contact with the abutment is defined by four design variables in four elevations, such as the crown cantilever. Coefficients, $k_r$ and $k_l$, determine the portion of the length of the arch with constant thickness on the right and left banks, respectively (Figure 3).

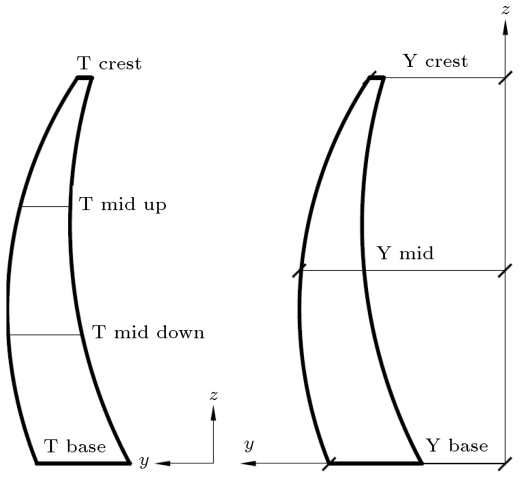


**Figure 2.** Design variables in crown cantilever.

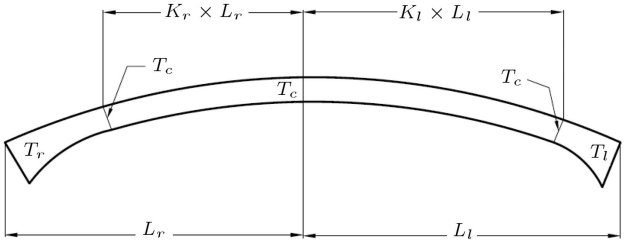


**Figure 3.** Design variables in horizontal section.

A parabolic function for the upstream face in the left and right segments of the dam are defined by assigning radius of curvature at the apex in three horizontal sections at the base, mid height and crest. Six variables are needed to determine these parabolas by the following relation:

$$y(x,z) = y_c - \frac{x^2}{2R(z)}, \tag{2}$$

where $R$ is the radius of the horizontal arch in $x = 0$, and $y_c$ determines the position of the center of the horizontal arch (Figure 4).

The last design variable is the angle of rotation of the dam around the $z$ axis (Figure 5).

In general, 30 design variables are used in the process of optimization as shown in Table 1.

### 2.2. Constraints

Geometric and stress constraints are two types of constraint which should be satisfied in the shape optimization of concrete arch dams [14]. Allowable stresses are the most important constraints in the design of concrete arch dams. Table 2 indicates allowable stresses and safety factors in concrete dams for different load combinations. Static unusual contains dead load and temperature load, and static usual contains Normal Water Level (NWL), dead load and concrete temperature occurring at NWL time. Static extreme is like static usual, but with the reservoir at Probable Maximum Flood (PMF) elevation [21].

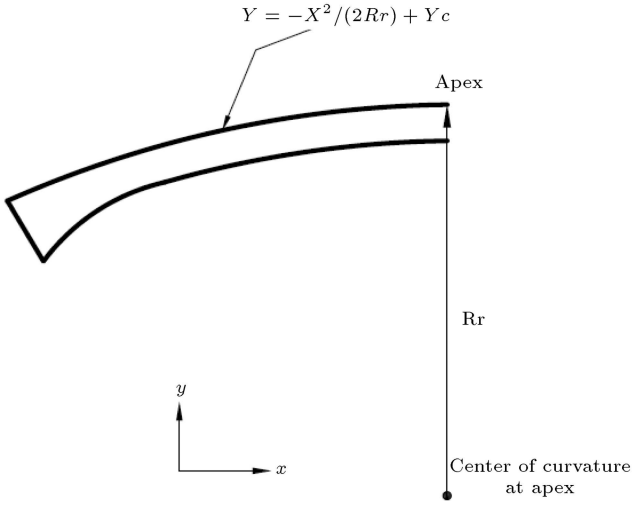


**Figure 4.** Radius of curvature of right bank.

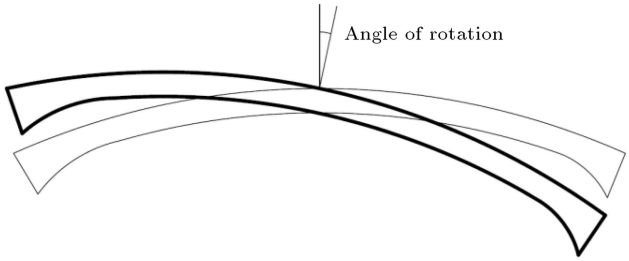


**Figure 5.** Angle of rotation of the horizontal arch.

In Table 2, $f'_c$ and $f'_t$ are the compressive and tensile strength of concrete, respectively. Tensile strength can be obtained from the Raphael formula [22]:

$$f'_t = \beta f_c^{\frac{2}{3}}. \tag{3}$$

If strength is in Pascal, and for actual tensile strength under static loading, $\beta$ equals 0.32 [22]. For example, if $f'_c = 25_{\text{MPa}}$, tensile strength is:

$$f'_t = 0.32 \times (25)^{(\frac{2}{3})} = 2.736_{\text{MPa}}.$$

Two geometric constraints are considered. The first is the minimum thickness at the crest ($T_{\min}$), according to the requirements of traffic and access of equipment to different locations of the crest during various stages of construction and operation. The second is the maximum vertical slope of the dam to facilitate construction (Figure 6):

$$T_c \geq T_{\min}, \tag{4}$$

$$s = \tan(\theta_{\max}) = \max(s_1, s_2) \leq 0.3. \tag{5}$$

**Table 1.** Design variables.

| | | | |
|---|---|---|---|
| Radius | R crest (right) | Thickness | T crest |
| | R mid (right) | | T mid up |
| | R base (right) | | T mid down |
| | R crest (left) | | T base |
| | R mid (left) | | T crest (right) |
| | R base (left) | | T mid up (right) |
| Coefficient | K crest (right) | | T mid down (right) |
| | K mid up (right) | | T base (right) |
| | K mid down (right) | | T crest (left) |
| | K base (right) | | T mid up (left) |
| | K crest (left) | | T mid down (left) |
| | K mid up (left) | | T base (left) |
| | K mid down (left) | Coordinate | Y crest (upstream) |
| | K base (left) | | Y mid (upstream) |
| | Rotation | | Y base (upstream) |

**Table 2.** Allowable stresses and factor of safety [21].

| Load combination | Allowable compressive stress | Allowable tensile stress | Factor of safety |
|---|---|---|---|
| Static usual | $f'_c/4$ | $f'_t$ | 2 |
| Static unusual | $f'_c/2.5$ | $f'_t$ | 1.3 |
| Static extreme | $f'_c/1.5$ | $f'_t$ | 1.1 |

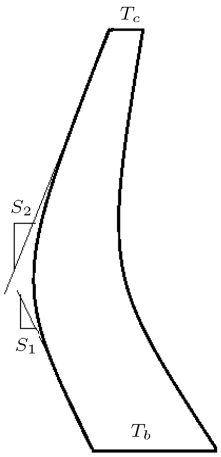


**Figure 6.** Geometric constraint.

## 3. Abutment stability in shape optimization

Stability of the abutment is one of the most important aspects in the stability analysis of arch dams [23], and is crucial to their safety. In abutment stability, we are concerned with the stability of the attached wedges which are in contact with the dam body. In this study, isolated wedges are not considered. To avoid sliding in the abutment, arch dam designers usually limit minimum slope, between the abutment and the valley bank, to 30 degrees [24], but, obviously, it is not sufficient.

The LONDE method [25] is an easy and fast method to assess the stability of abutment wedges under thrust and uplift forces. In this method, the wedges are considered rigid bodies, and the geometry of the wedges will not change during application of the forces throughout the investigation. Cohesion and tensile strength are usually neglected in the contact planes, and, therefore, it is supposed that the friction between surfaces is the only parameter that can resist against sliding. Moreover, it is supposed that the moments of the forces have negligible influences and can be ignored. After solving the 3D static equilibrium equation for applied forces, the factor of safety is obtained.

The applied forces to the wedges are the dam-rock interface, which can be obtained from finite element analysis, uplift pressure, the weight of wedges and resistance forces against sliding (Figures 7 and 8). The natural surfaces of wedges are generally irregular [25], but are assumed to be smooth, conservatively. Wedge geometry will be delimited by three planes, one of which will be a back-plane, and the other two, predominant geological formations in the rock structure [26].

Static equilibrium equations in three directions, $x$, $y$ and $z$, are solved to calculate the reaction forces acting on the planes. Due to equilibrium conditions and calculated plane reaction forces, eight cases of

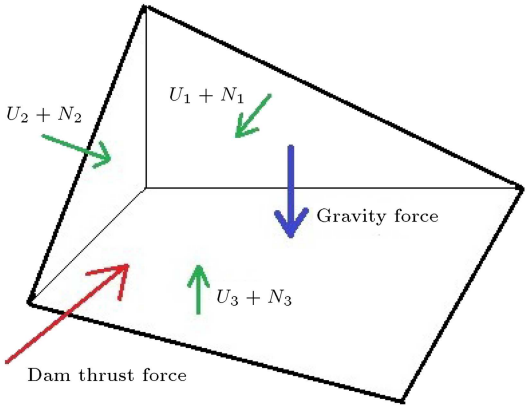


**Figure 7.** Typical three dimensional wedge arrangement.

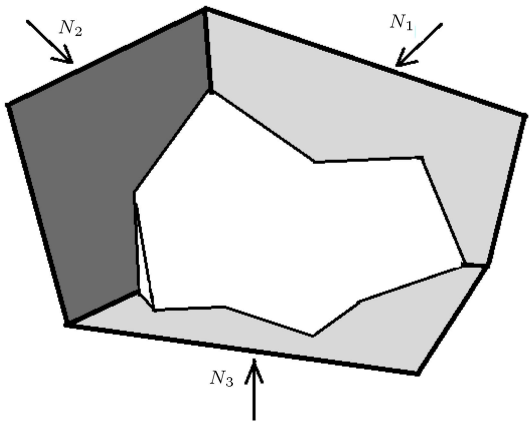


**Figure 8.** Normal contact forces.

**Table 3.** All possible movement of the wedge.

| Case | Nature of sliding | Contact forces | Open faces |
|---|---|---|---|
| 1 | No sliding | 1, 2, 3 | - |
| 2 | Intersection of plane 2, 3 | 2, 3 | 1 |
| 3 | Intersection of plane 1, 3 | 1, 3 | 2 |
| 4 | Intersection of plane 1, 2 | 1, 2 | 3 |
| 5 | In plane 3 | 3 | 1, 2 |
| 6 | In plane 2 | 2 | 1, 3 |
| 7 | In plane 1 | 1 | 2, 3 |
| 8 | In space | - | 1, 2, 3 |

sliding are possible (Table 3) [25]. For example, for case number 3 in Table 3, the factor of safety can be determined as follows:

$$\mathrm{SF} = \frac{s_{13}}{N_1 \tan\varphi_1 + N_3 \tan\varphi_3}, \tag{6}$$

$N_1$ and $N_3$ are normal contact forces for planes 1 and 3, $\varphi_1$ and $\varphi_3$ are the coefficient of internal friction and $S_{13}$ is the component of the sum of applied forces in the sliding direction.

A robust computer code is developed to find

the factor of safety for different wedge shapes under different load combinations.

## 4. Particle swarm optimization

Particle Swarm Optimization (PSO), which was originally proposed by Kennedy and Eberhart in 1995 [27], is a relatively new and robust optimization technique. It has attracted a great deal of attention in recent years due to its simplicity and efficiency [28].

Similar to other population based optimization algorithms, the PSO has two phases: initialization and evolution. In the initialization phase, the population is initialized with uniformly distributed random particles within their search space. In the evolution phase, particles search for the optimal by updating themselves based on their current and historic information until termination criteria are met.

Configuring the shape of the arch dam based on the design variables at every step of optimization has been determined as [29]:

$$P_i = [x_{i,1}, x_{i,2}, ..., x_{i,\mathrm{DV}}], \tag{7}$$

where $P_i$ is the vector of configuration and represents the $i$th shape of the dam, $x_{i,j}$ is the $j$th design variable, and index DV represents the number of design variables. During the evolution phase, the velocity of the $i$th particle is calculated as:

$$v_i(t) = v_i(t - \Delta t) + \alpha U_g(P_g - P_i) + \beta U_l(P_l - P_i), \tag{8}$$

where $P_l$ is the best previously visited position of particle $i$, $P_g$ is the global best position experienced by all particles in the history, and $\Delta t$ is the time interval in each step of the optimization. $\alpha$ and $\beta$ are randomly generated real numbers in the interval [0,1]. In addition, $U_g$ and $U_l$ are two positive constant parameters called acceleration factors. Next, the position of the $i$th point is updated by:

$$P_i(t + \Delta t) = P_i(t) + v_i \Delta t, \tag{9}$$

$\Delta t$ was decreased during optimization as:

$$\Delta t = c \times \Delta t, \tag{10}$$

where $c$ is a coefficient less than 1 [30].

The size of the population, which has been considered fixed throughout the optimization, has been $N_{\mathrm{pop}} = 10000$. Figure 9 shows the PSO processing flowchart.

## 5. Shape optimization procedure

Figure 10 represents the adopted shape optimization procedure. A computer code was developed to include

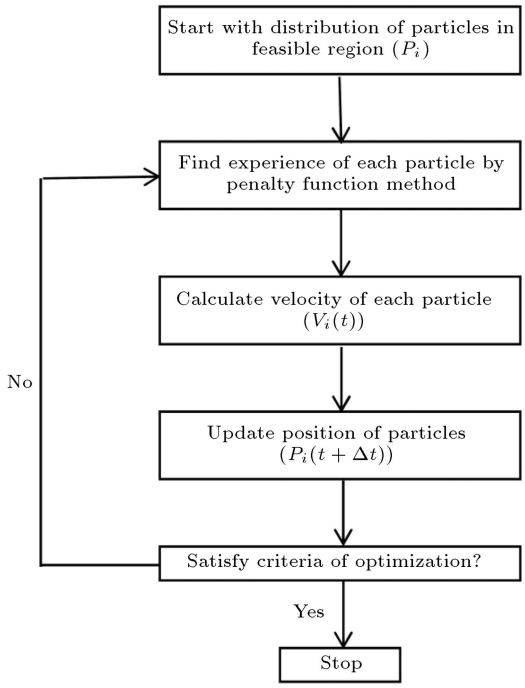


**Figure 9.** Flowchart of PSO method.

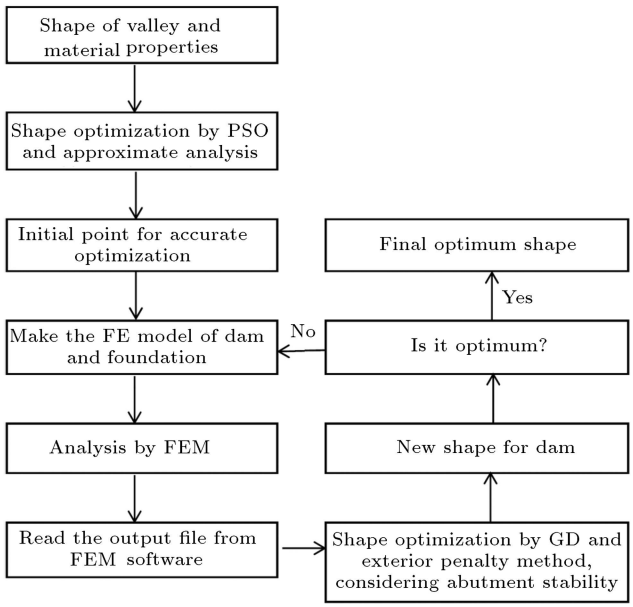


**Figure 10.** Shape optimization procedure.

the proposed procedure. In the first stage of optimization, Particle Swarm Optimization (PSO), based on an approximate method of analyzing concrete arch dams, is utilized to find the optimum shape [29]. The probability of finding global minimum in the PSO is high. This approach is merged with the approximate analysis of concrete arch dams proposed by Herzog [31] to decrease the time of the optimization process. The approximate analysis is shown to be entirely adequate by the posterior analysis of 60 arch dams. This stage ends up with an initial shape for the concrete

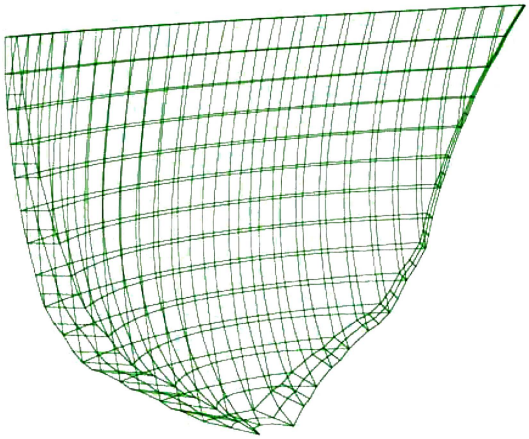

**Figure 11.** Finite element mesh of the dam body.

arch dam that will be used for the next stage of optimization.

In the next stage of optimization, the finite element mesh of the arch dam and abutment is made for the purpose of more accurate analysis using the finite element method.

The exterior penalty method is utilized to alter the constrained optimization problem to an unconstrained problem, and then, the steepest descent method is applied to solve the unconstrained problem [32].

Abutment stability analysis is considered in this stage of the analysis. This stage will end by finding the final optimum shape.

## 6. Finite element model

A computer code is written to prepare the input data for the finite element program and to read the output. A finite element mesh at a certain stage of the analysis for a dam-foundation system will be created. Figure 11 shows the finite element mesh generated by this code.

Two layers of iso-parametric 20-node elements, with 27 integration points and 8-node brick elements, are incorporated to idealize the dam and foundation, respectively. No self-weight effect is considered for the dam foundation by assuming zero gravity rock-mass. A relatively fine mesh is generated for the dam body (Figure 11). The maximum height and length of elements can be defined by designers. Foundation boundaries are taken parallel to the axes of the global coordinate system and have been extended to nearly 2 times the dam height, far away from the dam-foundation interface. Figure 12 shows the output model of dam foundation system.

The program has the ability to model thermal load as well. For this purpose, users must define the closure temperature in the dam body and the temperature of all nodes in air and water faces at different levels.

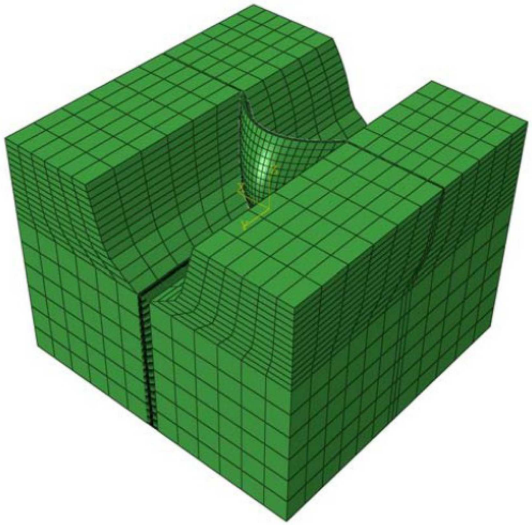

**Figure 12.** Finite element model of the dam and foundation.

### *6.1. Stage construction*

Large concrete arch dams are constructed from several blocks called monoliths. They are separated by vertical contraction joints filled with low tensile strength grouting material [33]. During construction, the maximum height of each block is usually 30 meters. Each stage is constructed in two sub-stages. In the first sub-stage, the odd cantilevers are erected, and in the next, the even cantilevers are built and the grouting is performed. The next stage of construction will be built on the deformed shape of previous stages.

In this research, the self weight of the dam is employed by a stage construction method, which represents a real practical situation. The maximum height of the grouting stages is limited to 25 m. It means that for a dam with a height of 200 m, at least 8 stages are incorporated. Stage construction is important in static analysis and needs to be considered for the shape optimization of concrete arch dams. Stress distribution under dead load will be wrong if stage construction is not considered in the model.

## 7. Stress concentration in static load combination

The results of analysis of several concrete arch dams with different valley shapes reveal that the values of maximum tensile stresses are usually high on the $U/S$ face for most static load combinations. Figure 13 represents the maximum principle stress more than 2.5 MPa in a dam body. These values lead to significantly high required concrete strengths. However, these values correspond to high tensile stresses at the dam foundation rock interface, which are somehow fictitious. These stresses occur in the arch direction, and, thus, are easily released by the opening of contraction joints at that

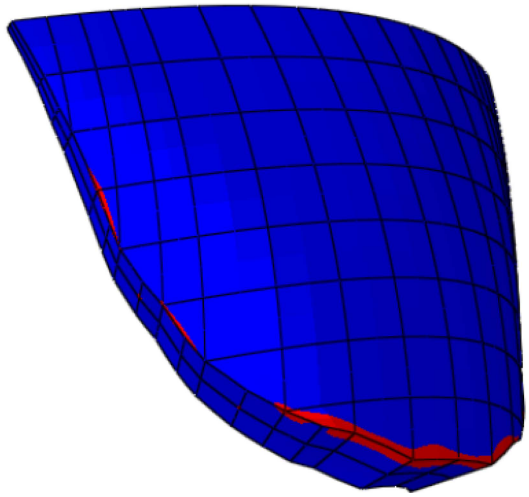

**Figure 13.** The maximum principal stress in dam.

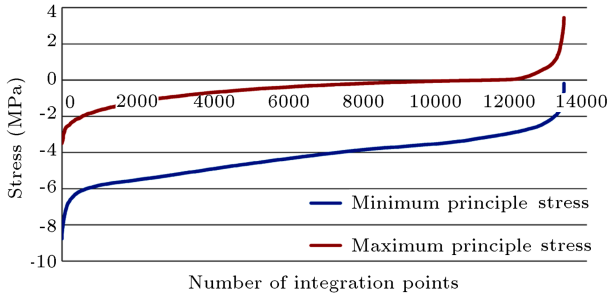


**Figure 14.** Sorted maximum and minimum principal stress in all integration points in the dam body.

location. In other words, they tend to be released as the corresponding joints open up.

There is not much concern for these high values of stress in these regions of concrete arch dams. This high value of stress may lead to high concrete volume if we try to satisfy allowable stresses in this region in the process of optimization. To overcome this problem, a methodology is proposed.

As shown in Figure 14, the integration points in the body of the dam with stress higher than the allowable tensile stress (say 2.5 MPa) are few. There are 13392 integration points in the finite element model of the dam and only 31 integration points have a maximum principle stress higher than the allowable tensile stress. To find a value to represent the high tensile stress in the dam body, the dimensionless function in Eq. (11) can be used as representative of the intensity and volume of overstress areas:

$$A = \frac{1}{V}\sum_{i=1}^{n}\frac{V_i}{p}\sum_{j=1}^{p}\max(0,\frac{\sigma_{i,j}-\sigma_{\text{all}}}{\sigma_{\text{all}}}), \qquad (11)$$

where $V$ represents the volume of the dam, $V_i$ is the volume of the $i$th element, $\sigma_{i,j}$ is the maximum principal stress in the $j$th integration point of the $i$th element, $n$ is the number of elements in the finite element model of the dam, $p$ is the number of integration points in each element, and $\sigma_{\text{all}}$ is the maximum allowable tension in the concrete.

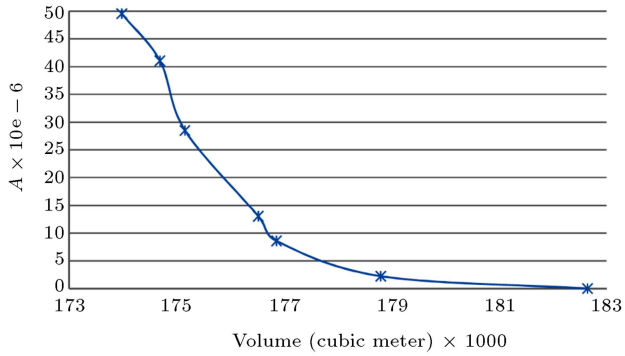


**Figure 15.** Pareto frontier for multi objective shape optimization of an arch dam.

In the optimization process, $A$ can be taken as a constraint, or, it can be used as the second objective function, and a multi-objective optimization process can be used to find the optimum volume and the $A$.

Multi-objective optimization with such conflicting objective functions gives rise to a set of optimal solutions instead of one optimal solution. Figure 15 represents the optimal volume, with respect to different values of $A$ for a dam. The reason for the optimality of many solutions is that no one solution can be considered to be better than any other, with respect to all objective functions. These optimal solutions have a special name: Pareto-optimal solutions [34]. Clearly, it can be observed that by using $A = 30 \times 10^{-6}$ instead of 0 for this dam, the volume decreases about 4.4%.

## 8. Results

A computer code is developed for shape optimization of concrete arch dams. The ability of the written code is tested by two examples. The first is a symmetric valley with one wedge in the left bank, and the second is an unsymmetrical valley with two wedges in the left and right banks.

### *8.1. Example 1*

A symmetric valley shape, such as Figure 16, is considered for the first example. The goal is to find the optimum shape for a concrete arch dam in this valley with a height of 150 m. The normal water level is 145 m.

The compression strength of the dam concrete, density, modulus of elasticity and Poisson's ratio are taken to be 25 MPa, 2400 kg/m$^3$, 24 GPa and 0.18, respectively. These parameters for the foundation rock are 8 GPa and 0.25 for the modulus of elasticity and Poisson's ratio, respectively. Table 4 shows the initial ranges for design variables.

Figure 17 represents changes in volume during the

**Table 4.** Initial ranges for design variables.

| | Min | Max | | Min | Max |
|---|---|---|---|---|---|
| R crest (right) | 0.4Lcrest=100 | 0.8Lcrest = 200 | T crest | 7 | 9 |
| R mid (right) | 0.4Lmid = 60 | 0.8Lmid = 150 | T mid up | 8 | 17 |
| R base (right) | 0.3Lmid = 45 | 0.6Lmid = 90 | T mid down | 10 | 20 |
| R crest (left) | 0.4Lcrest = 100 | 0.8Lcrest = 200 | T base | 0.1H=15 | 0.25H=37.5 |
| R mid (left) | 0.4Lmid = 60 | 0.8Lmid = 150 | T crest (right) | 7 | 14 |
| R base (left) | 0.3Lmid = 45 | 0.6Lmid = 90 | T mid up (right) | 8 | 25 |
| K crest (right) | 0.05 | 0.9 | T mid down (right) | 10 | 30 |
| K mid up (right) | 0.05 | 0.9 | T base (left) | 15 | 37.5 |
| K mid down (right) | 0.05 | 0.9 | T crest (left) | 7 | 14 |
| K base (right) | 0.05 | 0.9 | T mid up (left) | 8 | 25 |
| K crest (left) | 0.05 | 0.9 | T mid down (left) | 10 | 30 |
| K mid up (left) | 0.05 | 0.9 | T base (left) | 15.0 | 37.5 |
| K mid down (left) | 0.05 | 0.9 | Y crest (upstream) | 30 | 60 |
| K base (left) | 0.05 | 0.9 | Y mid (upstream) | 60 | 90 |
| Rotation (degree) | -10 | 10 | Y base (upstream) | 60 (fixed) | 60 |

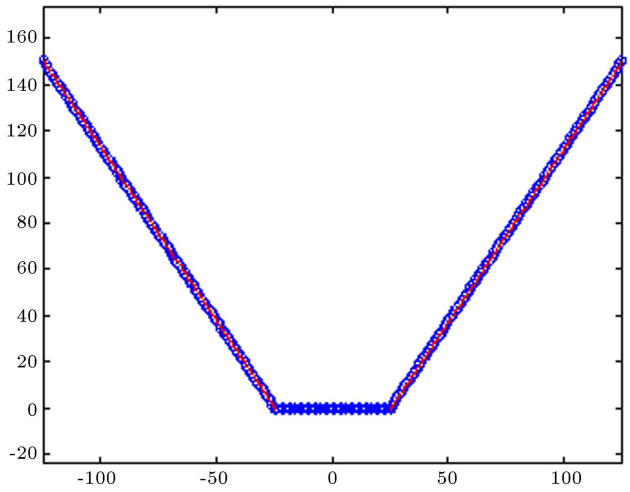


**Figure 16.** Shape of valley (meter).

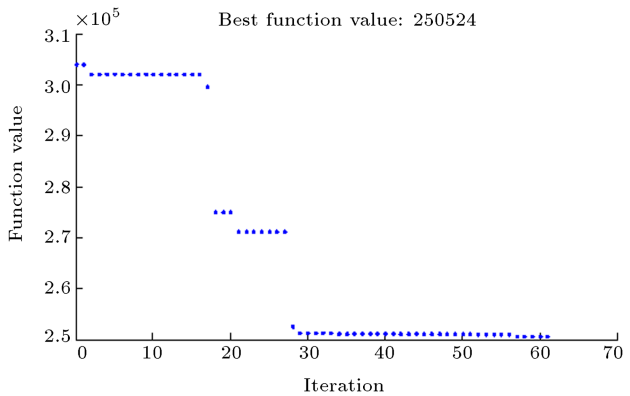


**Figure 17.** Volume changes during optimization process (second phase after approximate analysis).

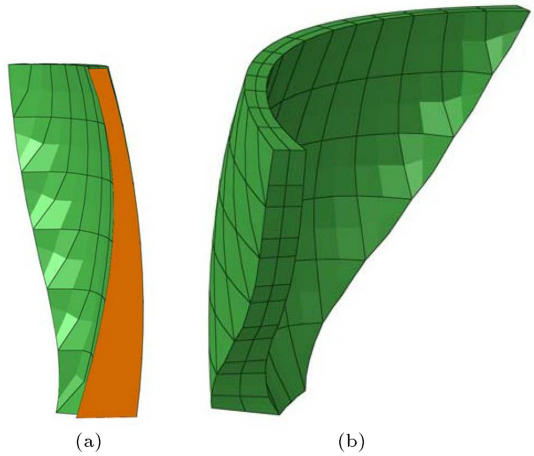


**Figure 18.** The optimum shape of dam: (a) Crown cantilever; and (b) 3D perspective.

optimization process. Figure 18 shows the optimum shape of the dam and Tables 5 and 6 are the output of data defining the final shape of the dam. As expected, the shape of the dam is symmetric. The final volume is 250524 $m^3$ and the final shape satisfied all constraints.

In Table 4, $R$ is the radius of curvature and $T$ is the thickness.

Figure 19 indicates the overhang and undercut on a crown cantilever. The boldness coefficient in Table 6 is a non dimensional indicative value calculated by Lombardi's formula, as Eq. (12):

$$\text{Boldness coefficient} = \frac{(\text{Mid surface area})^2}{H \times \text{Volume}}. \qquad (12)$$

Now, suppose there is a wedge in the left abutment (Figure 20). It is shaped with three surfaces defined in

**Table 5.** Properties of the dam body at various elevations.

| Elevation | R right | R left | T right | T center | T left | Y upstream | Y downstream |
|---|---|---|---|---|---|---|---|
| 0 | 51.65 | 51.65 | 27.47 | 25.23 | 27.47 | 60.00 | 29.77 |
| 25 | 47.10 | 47.10 | 19.68 | 18.90 | 19.68 | 64.53 | 45.63 |
| 50 | 50.85 | 50.85 | 15.43 | 12.63 | 15.43 | 66.72 | 54.09 |
| 75 | 62.88 | 62.88 | 13.77 | 9.91 | 13.77 | 66.56 | 56.65 |
| 100 | 83.20 | 83.20 | 13.09 | 9.25 | 13.09 | 64.05 | 54.81 |
| 125 | 111.82 | 111.82 | 12.14 | 9.15 | 12.14 | 59.20 | 50.05 |
| 150 | 148.71 | 148.71 | 9.99 | 8.12 | 9.99 | 52.00 | 43.89 |

**Table 6.** Properties of the dam body.

| | |
|---|---|
| Dam crest length (m) | 271.55 |
| Crest central angle (deg.) | 80.10 |
| Overhang (m) | 14.72 |
| Undercut (m) | 6.72 |
| Crest thickness (m) | 8.12 |
| Base thickness (m) | 25.23 |
| Max abut. thickness | 27.47 |
| Mid surface area ($m^2$) | 25976.35 |
| Volume ($m^3$) | 250524 |
| Boldness coefficient | 17.97 |

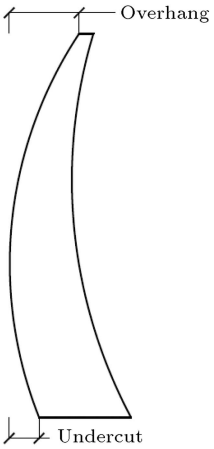


**Figure 19.** Undercut and overhang in the crown cantilever.

Table 7. The total mass of the wedge is 54000 ton and there is an uplift force on surface 1.

For the optimum shape from the previous step, the safety factor against sliding for the above wedge is 1.26, but, we need it to be more than the allowable value (say 2.0). Thus, to reach the desired safety factor for abutment stability, the obtained optimum shape is imported to code as the initial shape. The results show that considering this wedge, despite being a symmetric valley, leads to the asymmetric optimum shape, and it rotates about +8.43° (Figure 21 and Tables 8 and 9).

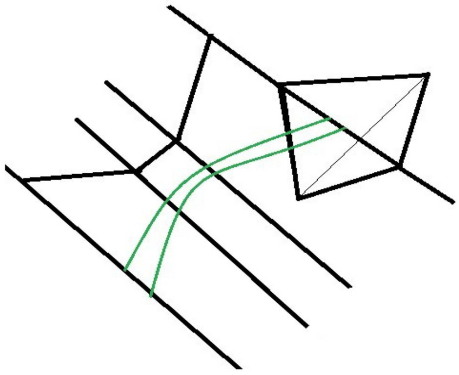

**Figure 20.** Wedge in left bank.

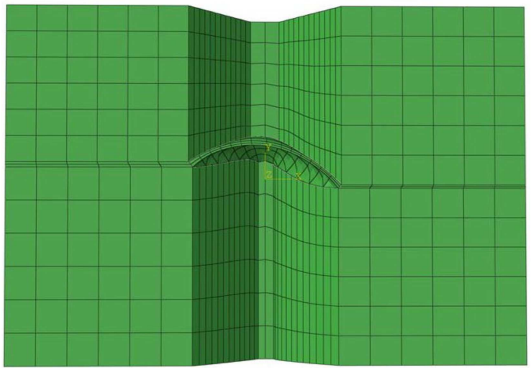

**Figure 21.** The optimum shape of dam considering abutment stability (horizontal view).

**Table 7.** Properties of the left wedge.

| | Surface 1 | Surface 2 | Surface 3 |
|---|---|---|---|
| **Dip direction** | 198.43 | 341.57 | 0 |
| **Dip angle** | 85.07 | 85.07 | 0 |
| $\phi$ | 40 | 30 | - |

The safety factor for the optimum shape is now more than 2.0.

As observed, the volume has increased by 5.19%, but, the dam is safe against sliding.

### *8.2. Example 2*

An unsymmetrical shape of a valley is considered (Figure 22). There are two wedges in the left and right

**Table 8.** Properties of the dam body at various elevations.

| Elevation | R right | R left | T right | T center | T left | Y upstream | Y downstream |
|---|---|---|---|---|---|---|---|
| 0 | 47.01 | 47.01 | 28.41 | 26.91 | 26.28 | 60.00 | 33.09 |
| 25 | 49.32 | 39.50 | 23.57 | 23.35 | 28.06 | 65.20 | 41.85 |
| 50 | 57.32 | 40.85 | 21.06 | 17.98 | 25.61 | 67.87 | 49.89 |
| 75 | 71.01 | 51.04 | 19.83 | 12.23 | 23.88 | 68.02 | 55.79 |
| 100 | 90.40 | 70.09 | 18.49 | 7.54 | 21.45 | 65.66 | 58.12 |
| 125 | 115.49 | 97.99 | 15.77 | 7.33 | 16.32 | 60.77 | 55.45 |
| 150 | 146.27 | 134.74 | 10.48 | 7.01 | 7.77 | 53.37 | 46.36 |

**Table 9.** Properties of the dam body.

| | |
|---|---|
| Dam crest length (m) | 274.78 |
| Crest central angle (deg.) | 81.13 |
| Overhang (m) | 14.66 |
| Undercut (m) | 8.02 |
| Crest thickness (m) | 7.01 |
| Base thickness (m) | 26.91 |
| Max abut. thickness | 28.41 |
| Mid surface area ($m^2$) | 25964.58 |
| Volume ($m^3$) | 263191 |
| Boldness coefficient | 17.08 |

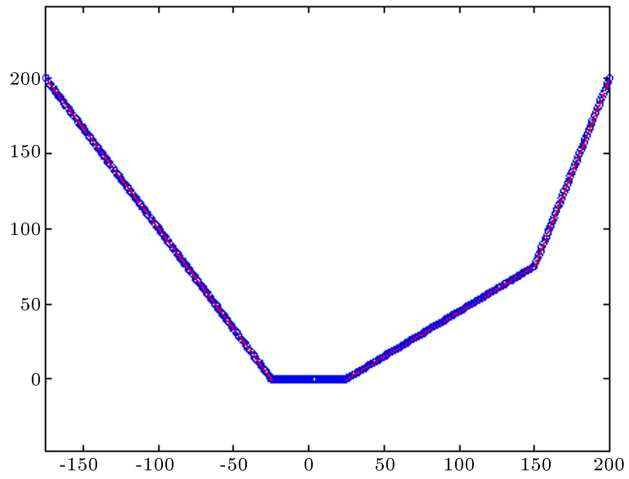


**Figure 22.** Shape of valley from downstream (meter).

banks (Table 10 and Figure 23), and the height of the dam and normal water level are 200 m and 190 m, respectively.

The properties of the bedrock and concrete are the same as the previous example. The result of the optimization process is given in Table 11. The final volume is 1279690 $m^3$, and the safety factor for both wedges in the optimum shape is more than 2.0. Moreover, the shape satisfies all other constraints, especially the maximum tensile stress constraint.

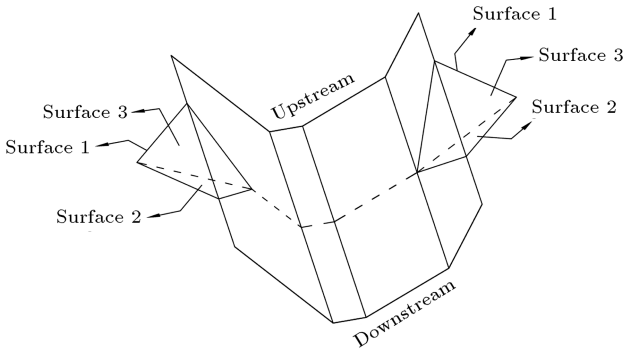


**Figure 23.** Geometry of wedges.

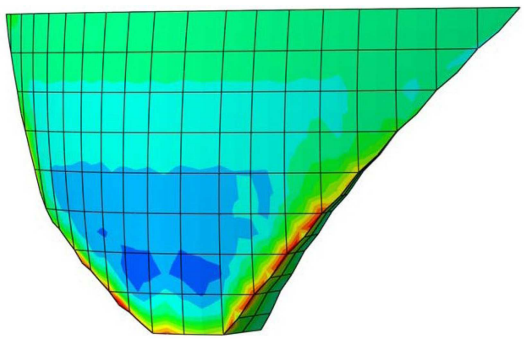

**Figure 24.** The maximum principal stress in the body of optimum shape of dam under STG+NWL.

Figure 24 shows the maximum principal stress in the optimum shape of a dam under dead load and hydrostatic pressure under a normal water level.

## 9. Conclusion

Shape optimization of a concrete arch dam is carried out using both a stress constraint and an abutment stability constraint. Considering abutment stability can change the optimum shape of arch dams and, usually, it is more important than tension stresses in the concrete arch dam body. A comprehensive code to model the arch dam and foundation, generate meshes, and calculate the stability of the wedges, is written. Using PSO in the optimization process increased the probability of finding the global optimum shape and

**Table 10.** Properties of wedges.

| | Left wedge | | | Right wedge | | |
|---|---|---|---|---|---|---|
| | **Surface 1** | **Surface 2** | **Surface 3** | **Surface 1** | **Surface 2** | **Surface 3** |
| **Dip direction** | 213.69 | 330.95 | 0 | 143.13 | 53.13 | 0 |
| **Dip angle** | 73.72 | 75.66 | 0 | 51.34 | 51.34 | 0 |
| $\phi$ | 40 | 35 | - | 40 | 30 | - |

**Table 11.** Design variables for the optimum shape.

| | | | | | |
|---|---|---|---|---|---|
| R crest (right) | 224.84 | T crest (right) | 9.63 | K crest (right) | 0.24 |
| R mid (right) | 173.44 | T mid up (right) | 29.23 | K mid up (right) | 0.63 |
| R base (right) | 112.95 | T mid down (right) | 45.34 | K mid down (right) | 0.15 |
| R crest (left) | 226.67 | T base (right) | 55.84 | K base (right) | 0.09 |
| R mid (left) | 178.79 | T crest (left) | 10.38 | K crest (left) | 0.44 |
| R base (left) | 94.70 | T mid up (left) | 26.58 | K mid up (left) | 0.46 |
| T crest | 9.07 | T mid down (left) | 30.75 | K mid down (left) | 0.54 |
| T mid up | 22.17 | T base (left) | 47.96 | K base (left) | 0.07 |
| T mid down | 41.02 | Rotation | -9.69 | Y crest (upstream) | 52.02 |
| T base | 48.33 | Y base (upstream) | 60 (fixed) | Y mid (upstream) | 61.42 |

it can be fast when PSO is merged with approximate analysis. The performance of the code is checked by several valley and wedge shapes. A novel dimensionless function is introduced. The written code can use this function as another objective function or as a constraint to reduce the final volume of the concrete arch dam.

## References


1. Rajan, M.K.S., *Shell Theory Approach for Optimization of Arch Dam Shapes.*, University of California, Berkeley (1968).
2. Sharpe, R. "The optimum design of arch dams", *Proceedings of the ICE - Civil Engineering*, Supplementary Volume, pp. 73-98 (1969).
3. Mohr, G.A. "Design of shell shape using finite elements", *Computers & Structures*, **10**(5), pp. 745-749 (1979).
4. Sharma, R. "Optimal configuration of arch dams", Ph.D Thesis, Indian Institute of Technology, Kanpur (1983).
5. Wasserman, K. "Three dimensional shape optimization of arch dams with prescribed shape function", *Journal of Structural Mechanics*, **11**(4), pp. 465-489 (1984).
6. Bofang, Z. "Shape optimization of arch dams", **39**, Dartford, ROYAUME-UNI, Wilmington Business Publishing, 7, pp. 43-51 (1987).
7. Bofang, Z. "Optimum design of arch dams", *Dam Engineering*, **1**(2), pp. 131-145 (1990).
8. Bofang, Z., Rao, B., Jia, J. and Li, Y. "Shape optimization of arch dams for static and dynamic loads", *Journal of Structural Engineering*, **118**(11), pp. 2996-3015 (1992).
9. Maheri, M., Taleb-Beydokhti, N. and Ahadi, S. "Shape optimisation of concrete arch dams using simple genetic algorithm", *Dam Engineering*, **14**(2), pp. 105-140 (2003).
10. Peng, H., Yao, W. and Huang, P., *The Closure Temperature Fields and Shape Optimization of Arch Dam Based on Genetic Algorithms, in High Performance Computing and Applications*, W. Zhang, et al., Editors. Springer Berlin Heidelberg. pp. 317-324 (2010).
11. Kaveh, A. and Mahdavi, V. "Optimal design of arch dams for frequency limitations using charged system search and particle swarm optimization", *International Journal of Optimization in Civil Engineering*, **4**, pp. 543-555 (2011).
12. Seyedpoor, S.M., Salajegheh, J., Salajegheh, E. and Gholizadeh, S. "Optimal design of arch dams subjected to earthquake loading by a combination of simultaneous perturbation stochastic approximation and particle swarm algorithms", *Applied Soft Computing*, **11**(1), pp. 39-48 (2011).
13. Gholizadeh, S. and Seyedpoor, S.M. "Shape optimization of arch dams by metaheuristics and neural networks for frequency constraints", *Scientia Iranica*, **18**(5), pp. 1020-1027 (2011).
14. Akbari, J., Ahmadi, M.T. and Moharrami, H. "Advances in concrete arch dams shape optimization",

*Applied Mathematical Modelling*, **35**(7), pp. 3316-3333 (2011).

15. Akbari, J., Kim, N. and Ahmadi, M.T. "Shape sensitivity analysis with design-dependent loadings-equivalence between continuum and discrete derivatives", *Structural and Multidisciplinary Optimization*, **40**(1-6), pp. 353-364 (2010).
16. Seyedpoor, S.M., Salajegheh, J. and Salajegheh, E. "Shape optimal design of arch dams including dam-water-foundation rock interaction using a grading strategy and approximation concepts", *Applied Mathematical Modelling*, **34**(5), pp. 1149-1163 (2010).
17. Sun, L., Zhang, W. and Xie, N. "Multi-objective optimization for shape design of arch dams", in *Computational Methods in Engineering & Science*, Springer Berlin Heidelberg, pp. 299-299 (2007).
18. Zhang, X.-f., Li, S.-y. and Chen, Y.-l. "Optimization of geometric shape of Xiamen arch dam", *Advances in Engineering Software*, **40**(2), pp. 105-109 (2009).
19. Li, S., Ding, L., Zhao, L. and Zhou, W. "Optimization design of arch dam shape with modified complex method", *Advances in Engineering Software*, **40**(9), pp. 804-808 (2009).
20. Serafim, J.L. and Clough, R.W., *Arch Dams: International Workshop on Arch Dams*, Coimbra, 5-9 April 1987, AA Balkema (1990).
21. Engineers, U.S.A. C.o., *Arch Dam Design.*, Washington, DC (1994).
22. Raphael, J.M. "Tensile strength of concrete", in *ACI Journal Proceedings*, ACI (1984).
23. Sohrabi, M., Feldbacher, R. and Zenz. G. "Stability of dam abutment including seismic loading", in *Benchmark Workshop on Dam Analysis*, Paris (2009).
24. Samy, M. and Wieland, M. "Shape optimization of arch dams for static and dynamic loads", in *Proc. International Workshop on Arch Dams*, Coimbra (1987).
25. Londe, P., "Analysis of the stability of rock slopes", *Quarterly Journal of Engineering Geology and Hydrogeology*, **6**(1), pp. 93-124 (1973).
26. Stucky, "Theme C, stability of a dam abutment including seismic loading", in *Tenth Benchmark Workshop on Numerical Analysis of Dams*, ICOLD, Ankara (2009).
27. Eberhart, R.C. and Kennedy, J. "A new optimizer using particle swarm theory", in *Proceedings of the Sixth International Symposium on Micro Machine and Human Science*, New York, NY (1995).
28. Clerc, M. "Particle swarm optimization", France, Wiley-ISTE (2006).
29. Takalloozadeh, M. and Ghaemian. M. "Approximate optimum shape of concrete arch dam using particle swarm optimization", in *The First International Conference on Dams & Hydro Powers*, Tehran, Iran (2012).
30. Parsopoulos, K.E. and Vrahatis, M.N. "Particle swarm optimization and intelligence: advances and applications", Information Science Reference Hershey (2010).
31. Herzog, M. *Practical Dam Analysis*, Thomas Telford (1999).
32. Rao, S.S., *Engineering Optimization: Theory and Practice*, NewAge International (P) Limited, Publishers (1996).
33. Tzenkov, A.D., *Seismic Modelling and Analysis of Concrete Arch Dams with Contraction Joints and Nonlinear Concrete Material Models* (2001).
34. Sarker, R., Mohammadian, M. and Yao, X., *Evolutionary Optimization*, **48**, Springer (2002).

## Biographies

**Meisam Takalloozadeh** is a PhD degree candidate in the Civil Engineering Department of Sharif University of Technology, Tehran, Iran. His research interests are mathematical methods in optimization, and shape and topology optimization of structures. In recent years, he has been working on shape optimization of concrete dams.

**Mohsen Ghaemian** is Associate Professor in the Civil Engineering Department of Sharif University of Technology, Tehran, Iran. His current research activities include dynamic responses of gravity and arch dams, dam reservoir interaction effects, seismic response of dams due to non-uniform excitations, and nonlinear behavior of concrete dams.